6-15-2012

Focal Adhesion Kinase Modulates Cdc42 Activity Downstream of Positive and Negative Axon Guidance Cues

Jonathan P. Myers
University of Wisconsin-Madison

Estuardo Robles
Max-Planck-Institut für Neurobiologie, erobles@smith.edu

Allison Ducharme-Smith
University of Wisconsin-Madison

Timothy M. Gomez
University of Wisconsin-Madison

Focal adhesion kinase modulates Cdc42 activity downstream of positive and negative axon guidance cues

Jonathan P. Myers[1,*], Estuardo Robles[2,*], Allison Ducharme-Smith[1] and Timothy M. Gomez[1,‡]

[1]Department of Neuroscience, Medical Scientist Training Program and Neuroscience Training Program, University of Wisconsin, Madison, WI 53706, USA
[2]Max-Planck Institute for Neurobiology, Martinsried, Germany

*These authors contributed equally to this work
‡Author for correspondence (tmgomez@wisc.edu)

Accepted 17 January 2012
Journal of Cell Science 125, 2918–2929

doi: 10.1242/jcs.100107

Summary

There is biochemical, imaging and functional evidence that Rho GTPase signaling is a crucial regulator of actin-based structures such as lamellipodia and filopodia. However, although Rho GTPases are believed to serve similar functions in growth cones, the spatiotemporal dynamics of Rho GTPase signaling has not been examined in living growth cones in response to known axon guidance cues. Here we provide the first measurements of Cdc42 activity in living growth cones acutely stimulated with both growth-promoting and growth-inhibiting axon-guidance cues. Interestingly, we find that both permissive and repulsive factors can work by modulating Cdc42 activity, but in opposite directions. We find that the growth-promoting factors laminin and BDNF activate Cdc42, whereas the inhibitor Slit2 reduces Cdc42 activity in growth cones. Remarkably, we find that regulation of focal adhesion kinase (FAK) activity is a common upstream modulator of Cdc42 by BDNF, laminin and Slit. These findings suggest that rapid modulation of Cdc42 signaling through FAK by receptor activation underlies changes in growth cone motility in response to permissive and repulsive guidance cues.

Key words: Axon guidance, Pathfinding, Neural development

Introduction

Neuronal growth cones must respond rapidly and accurately to extracellular cues to navigate to their proper synaptic targets. Changes in the dynamics of filopodia and lamellipodial protrusions underlie many growth cone pathfinding behaviors (reviewed by Kater and Rehder, 1995; Dent and Gertler, 2003; Dent et al., 2011). Membrane protrusion is controlled by regulated actin polymerization at the growth cone leading edge, suggesting that guidance cues act by modulating the activity of cytoskeletal regulatory proteins (Gallo and Letourneau, 2004). Cdc42 is a member of the Rho-family of GTPases that probably serves this function through several effectors that regulate the actin cytoskeleton (reviewed by Meyer and Feldman, 2002). Consistent with this possibility, Cdc42 mediates BDNF-induced growth cone chemoattraction (Yuan et al., 2003) and Slit-induced repulsion of neuronal migration (Wong et al., 2001). Although these studies have implicated Cdc42 as a signaling component downstream of TrkB and Robo receptors, the upstream modulators of Cdc42 are largely unknown. Additionally, the spatial and temporal dynamics of Cdc42 activity within growth cones in response to these guidance cues has not been explored.

Fluorescent biosensors of active Rho GTPases have been used to show that Rho GTPase activity is elevated in the peripheral lamellipodia of motile non-neuronal cells (Kurokawa et al., 2004; Nalbant et al., 2004; Machacek et al., 2009). Probes using fluorescence resonance energy transfer (FRET) have demonstrated that Cdc42 activity rapidly increases within the peripheral lamellipodia of Cos1 cells following stimulation with epidermal growth factor (Kurokawa et al., 2004). Similarly, Nalbant and colleagues (Nalbant et al., 2004) have reported activation of endogenous Cdc42 in the peripheral lamellipodia of fibroblasts during cell adhesion and spreading. More recent work compared the activity of Cdc42, Rac1 and RhoA in extending and retracting lamellipodia of fibroblasts (Machacek et al., 2009). However, it remains unclear whether local and dynamic modulation of Cdc42 activity correlates with growth cone protrusions in response to naturally occurring axon guidance cues. Several studies have suggested that the direction of growth cone motility can be controlled by asymmetrical distribution of lamellipodia and filopodia (Bentley and O'Connor, 1994; Fan and Raper, 1995; Zheng et al., 1996), thus, this issue is of central importance to axon pathfinding. Regulation of lamellipodial and filopodial dynamics by local Cdc42 modulation could represent an important mechanism linking guidance cue receptor activation to changes in growth cone motility.

In this study we demonstrate that the guidance cues BDNF and Slit, as well as the extracellular matrix molecule laminin, regulate growth cone morphology and motility in a FAK- and Cdc42-dependent manner. Live imaging of Cdc42 activity using a fluorescent biosensor revealed that increased Cdc42 activity at the growth cone periphery correlates with the protrusion of both lamellipodia and filopodia. Furthermore, acute stimulation with BDNF or laminin strongly increased protrusion and Cdc42 activity in lamellipodia and filopodia. Conversely, Slit application rapidly reduced protrusion and Cdc42 activity at the growth cone periphery. Interestingly, we found that regulation of

FAK activity corresponded closely with Cdc42 in response to BDNF, laminin and Slit, and that disrupting FAK function interfered with Cdc42 modulation downstream of these guidance cues. These findings demonstrate that axon guidance cues regulate neuronal morphology and motility by controlling Cdc42-dependent actin dynamics downstream of FAK at the leading edge of the growth cone.

Results

BDNF potentiates lamellipodial dynamics in a Cdc42-dependent manner

Cdc42 activity assays from cell extracts suggest that BDNF and laminin increase active Cdc42 in developing neurons, whereas Slit decreases the level of active Cdc42 (Weston et al., 2000; Wong et al., 2001; Yuan et al., 2003), but nothing is known about the spatial or temporal dynamics of Cdc42 signals within living growth cones. To first test whether Cdc42 is required downstream of BDNF to promote changes in growth cone motility, we examined *Xenopus* spinal neuron growth cones expressing either GFP or GFP–DN-Cdc42 cultured on poly-D-lysine (PDL) (supplementary material Fig. S1A–L). PDL provides basal conditions where many neurons extend short axons with small and unstable protrusions for comparison with stimulated conditions. Addition of control medium to GFP–expressing neurons resulted in only a small change in growth cone area after 10 minutes. However, after 10 minutes of BDNF stimulation, GFP-expressing neurons underwent a significant increase in growth cone area that was largely due to the generation of new peripheral lamellipodia (supplementary material Fig. S1D,E). By contrast, DN-Cdc42-expressing growth cones, which typically had few lamellipodia before stimulation, did not exhibit a significant change in growth cone area after BDNF treatment (supplementary material Fig. S1J,K).

To confirm that changes in growth cone morphology were due to altered lamellipodial protrusion, we quantified membrane protrusion by kymography over a 10 minute interval before stimulation and 5–15 minutes following application of either BDNF or laminin. We used laminin as an alternative stimulant because it has previously been shown to signal through Cdc42 (Brown et al., 2000). Single-line kymographs were constructed over active lamellipodial regions to measure the size of individual protrusion events during each time interval (before and after application of laminin or BDNF; see the Materials and Methods for details) (supplementary material Fig. S1C,F–I). The sum of these events yielded the total membrane protrusion, which we expressed as a function of time. Using this method, we found that wild-type neurons exhibited a robust increase in membrane protrusion within 5 minutes of bath application of laminin, and often resulted in accelerated outgrowth (supplementary material Fig. S1A–C,L). Stimulation with BDNF also produced a strong increase in protrusion (supplementary material Fig. S1D–G,L). Examination of DN-Cdc42-expressing growth cones revealed a significant reduction in baseline lamellipodial protrusion compared with control growth cones (supplementary material Fig. S1L), confirming that endogenous Cdc42 activity promotes lamellipodial protrusion on PDL. Furthermore, DN-Cdc42-expressing growth cones did not exhibit a significant change in membrane protrusion following BDNF stimulation (supplementary material Fig. S1H–L). Together, these findings suggest that the growth-promoting effects of BDNF and probably laminin are due to Cdc42-dependent potentiation of lamellipodial protrusion dynamics.

Slit inhibition of lamellipodial protrusion requires downregulation of Cdc42 activity

Slit has been shown to repel migrating neurons in a Cdc42-dependent manner (Wong et al., 2001); however, it is unknown whether this effect is due to altered leading edge protrusion. To test this possibility, we examined the effects of *Xenopus* Slit stimulation on lamellipodial dynamics in growth cones expressing either GFP or GFP–CA-Cdc42. In these experiments, spinal neurons were cultured from stage 28 *Xenopus* embryos, because older neurons were found to be more sensitive to Slit2 (Stein and Tessier-Lavigne, 2001). In our initial studies, we used *Xenopus* Slit (xSlit), the *Xenopus* homologue of murine Slit2, purified from HEK cell-conditioned medium. We quantified membrane protrusion by kymography over 10 minute intervals before and following application of xSlit. Membrane protrusions from wild-type neurons were completely suppressed immediately following xSlit stimulation (supplementary material Fig. S1M,N,Q,S). By contrast, CA-Cdc42-expressing growth cones did not exhibit a statistically significant change in membrane protrusion following xSlit application (supplementary material Fig. S1O,P,R,S). Together, these findings suggest that the repulsive effects of Slit are due to reduced Cdc42 activity in growth cones causing the acute inhibition of lamellipodial protrusion.

Slit2 inhibition of outgrowth requires inactivation of FAK

We have previously shown that activation of Src and focal adhesion kinase (FAK) are necessary for the growth-promoting effects of BDNF on *Xenopus* spinal neuron growth cones (Robles et al., 2005; Myers and Gomez, 2011). Because Slit has the opposite effect on growth cone behavior compared with BDNF, we reasoned that it might be due to inactivation of FAK. To test whether the effects of Slit require modulation of FAK activity, we examined neurons expressing constitutively active SuperFAK (Gabarra-Niecko et al., 2002). Owing to the uncertainty of the *Xenopus* Slit concentration in our HEK-conditioned medium, we switched to a commercial source of murine Slit2 with a defined concentration (see the Materials and Methods) and examined the dose-dependent effects of Slit2 on axon extension. Murine Slit2 has previously been shown to be an effective inhibitor of *Xenopus* spinal neurons (Stein and Tessier-Lavigne, 2001). For some experiments, neurons were cultured on laminin to promote rapid axon extension and provide a sensitive assay to test the dose-dependent effects of Slit2. We found that bath application of Slit2 caused a dose-dependent inhibition of axon outgrowth by spinal neurons cultured at stage 28, with higher doses of Slit2 causing many neurons to retract (Fig. 1A–D). Similar to previous results, we found that spinal neurons cultured from young embryos were less sensitive to Slit2 (Stein and Tessier-Lavigne, 2001), which is consistent with commissural interneurons gaining sensitivity to Slit2 after midline crossing. Interestingly, expression of a constitutively active mutant of FAK, termed SuperFAK (Gabarra-Niecko et al., 2002) reduced the inhibitory effects of Slit2. To test whether changes in growth cone area induced by Slit2 were also attenuated by SuperFAK, we examined neurons fixed after a 5 minute treatment with 50 ng/ml Slit2 (Fig. 1E–H). Quantification of growth cone area from thresholded phalloidin fluorescence, which labels F-actin, showed decreased growth cone area after Slit2 treatment in wild-type neurons ($89\pm8.9\ \mu m^2$ to $43\pm4.7\ \mu m^2$), but little change in growth cone area by SuperFAK expressing neurons ($109\pm15\ \mu m^2$ to $102\pm13\ \mu m^2$). Similar results were also found

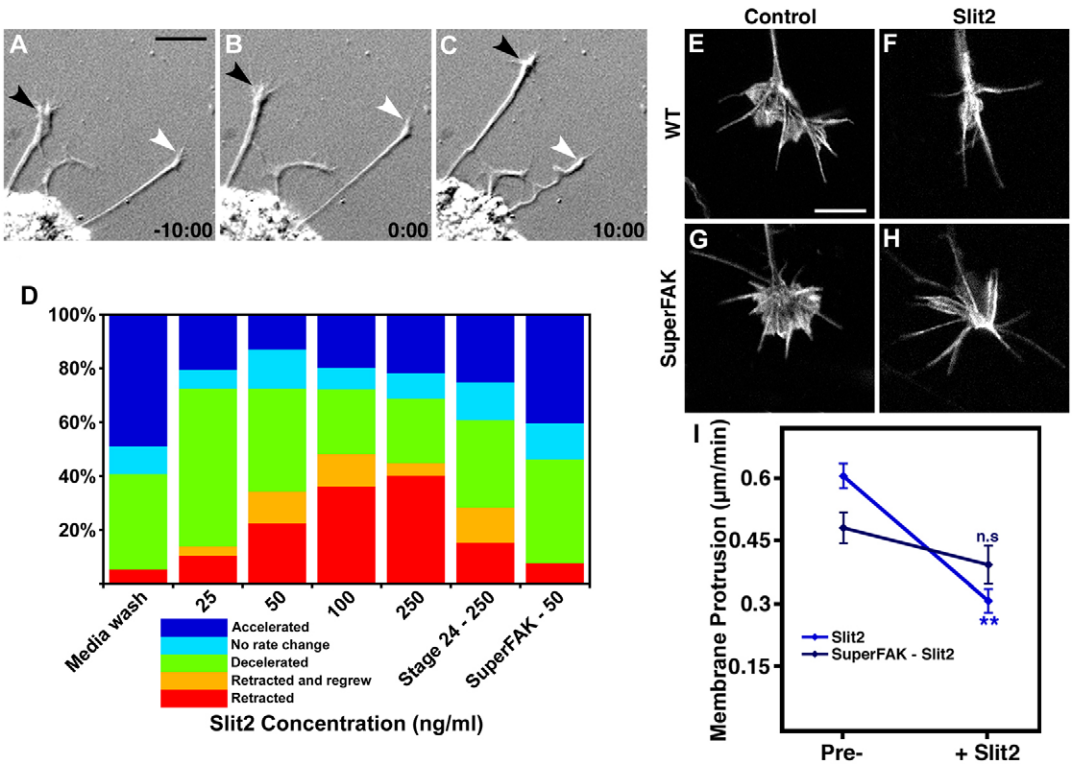

Fig. 1. Slit2 induces collapse and deceleration through FAK. (**A–C**) Time-lapse DIC images of *Xenopus* spinal neuron growth cones showing the response to 100 ng/ml Slit2 at the times indicated. Note that some neurons retract in response to Slit2 (white arrowhead), whereas others appear insensitive (black arrowhead), which is probably due to multiple classes of neurons in spinal cord explant cultures. Scale bar: 20 µm. (**D**) Categorical bar graph showing the effects of increasing doses of Slit2 on axon behavior of wild-type stage 28 neurons, as well as neurons cultured from stage 24 embryos and SuperFAK expressing neurons cultured at stage 28. Note the shift from deceleration to retraction at increasing doses of Slit2, and the reduced response in young and SuperFAK expressing neurons. $n \geq 59$ for each condition. (**E–H**) Wild-type and SuperFAK-expressing growth cones labeled with fluorescent phalloidin to show F-actin in control and treated neurons (50 ng/ml Slit2). (**I**) Quantification of changes in protrusion 10 minutes before and 10 minutes after Slit2 application in control and SuperFAK-expressing growth cones. Note reduced basal protrusive activity in SuperFAK neurons, but also muted effects of Slit2 stimulation. $^{**}P<0.0001$ by Student's *t*-test. $n=20$ growth cones measured before and after stimulation for each condition. Scale bar: 5 µm.

by protrusion analysis of neurons cultured on PDL. Bath application of 250 ng/ml Slit2 resulted in a sharp drop in growth cone protrusion, which was suppressed in SuperFAK-expressing neurons exposed to Slit2 (Fig. 1I). Together these findings suggest that Slit2 inhibits lamellipodial protrusion and axon outgrowth, in part through inactivation of FAK.

Slit2 inactivates FAK and Src

To directly assess how Slit2 influences FAK and Src signaling, we examined neurons treated with 50 ng/ml Slit2 by quantitative immunocytochemistry (ICC) using phospho-specific antibodies against FAK and Src. Activation of FAK and Src is associated with autophosphorylation at Y397 and Y418, respectively (Schaller et al., 1994; Thomas and Brugge, 1997), which occurs downstream of numerous axon guidance cues (Li et al., 2004; Liu et al., 2004; Ren et al., 2004; Bechara et al., 2008; Woo et al., 2009). By contrast, here we found that treatment of neurons on laminin for 5 minutes with Slit2 leads to a strong inactivation of FAK, as indicated by reduced tyrosine phosphorylation at both Y397 and Y861 (Fig. 2A,B,E). The Y861 site on FAK provides a binding site for several downstream proteins, including p130Cas (Mitra et al., 2005), which has been shown to modulate Rac1 and Cdc42 signaling downstream of FAK (Liu et al., 2007). Slit2 also inactivated Src, as indicated by a decrease in Y418 phosphorylation (Fig. 2C–E). As a negative regulator of Src, Csk phosphorylates the C-terminal Y529 of Src, which promotes an auto-inhibited confirmation (Okada and Nakagawa, 1989; Thomas and Brugge, 1997). Consistent with the inactivation of Src, we found that tyrosine phosphorylation at Y529 of Src was increased in growth cones treated with Slit2 (Fig. 2E; supplementary material Fig. S2).

We have previously reported that BDNF and EphrinA1 activate FAK and Src in growth cones cultured on laminin (Woo et al., 2009; Myers and Gomez, 2011), but EphrinA1 cannot activate FAK in growth cones cultured on PDL (Woo et al., 2009). To test the necessity for integrin engagement for this aspect of the response to BDNF, we cultured neurons on PDL, stimulated with BDNF for 10 minutes, and performed immunocytochemistry as described previously. Unlike EphrinA1, BDNF was able to further stimulate FAK and Src activities without integrin engagement (Fig. 2F). Laminin provides a strong stimulus to FAK and Src activation in many cell types (Hynes, 2002), but the exact phosphorylation state in growth cones acutely stimulated with laminin has not been tested. Neurons cultured on PDL showed a high degree of FAK and Src activation after treatment with laminin for 10 minutes (Fig. 2G). Importantly, the pattern of phosphorylation closely mimicked that seen with BDNF stimulation, and both showed opposite

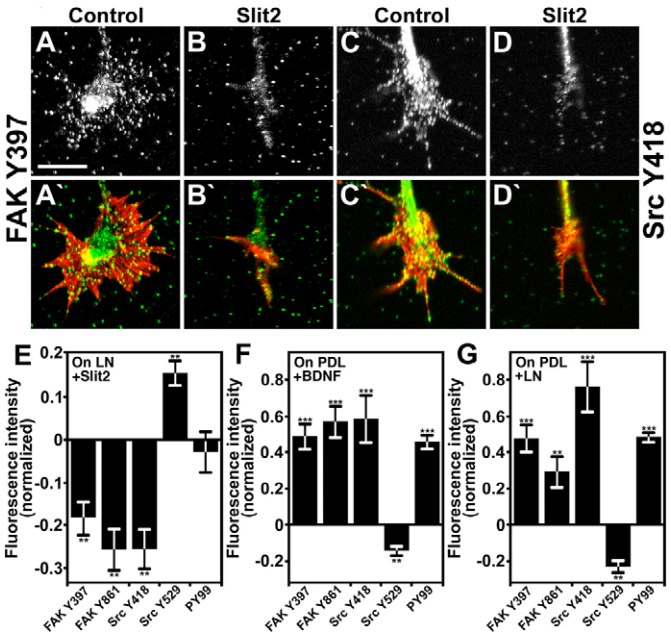

Fig. 2. Slit2 inactivates FAK and Src in neurons cultured on laminin. (**A–D**) Control and Slit2-treated neurons on laminin, fixed and stained with phospho-specific antibodies against Y397 FAK and Y418 Src. (**A′–D′**) Merged images of immunolabeled growth cones in A–D (green) merged with F-actin (red). (**E–G**) Quantification of fluorescence intensity in neurons on laminin stimulated for 5 minutes with 50 ng/ml Slit2 or BDNF, and neurons on PDL stimulated for 10 minutes with laminin, normalized to unstimulated growth cones. Note the opposing effects of Slit2 compared with BDNF and laminin. $n \geq 40$ growth cones per condition. ***$P<0.0001$, **$P<0.001$ compared with unstimulated control by Student's *t*-test. Scale bar: 5 μm.

changes compared with Slit2 stimulation. These data suggest that laminin, BDNF and Slit2 regulate growth cone motility and signaling through FAK and Src in a reciprocal fashion to guide axon outgrowth. Importantly, the changes in FAK pY861 mirror the changes seen in growth cone protrusion, indicating that these cues signal through FAK to modulate p130Cas, which can activate Cdc42 and Rac1.

Live imaging of Cdc42 activity in neuronal growth cones

Our findings suggest that guidance cues control protrusion by modulating Cdc42 activity at the growth cone periphery. To determine the spatial distribution of active Cdc42 in live cells, we used a biosensor containing GFP fused to the GTPase-binding-domain from WASP (wGBD), which specifically binds to active Cdc42 (Sokac et al., 2003). In our initial examination, we cultured GFP–wGBD-expressing neurons on laminin, which strongly promotes growth cone motility through activation of Cdc42 (Weston et al., 2000). It is important to note that the expression of GFP–wGBD in neurons was carefully titrated to levels that did not alter normal neurite outgrowth. Regions of elevated Cdc42 activity were identified by collecting ratio images of GFP–wGBD fluorescence relative to tetramethylrhodamine–dextran (TMR-D), which is used to normalize for cell volume. Most images were collected by total internal reflection fluorescence (TIRF) microscopy, which is optimal since Rho GTPases translocate to the membrane upon activation (Bokoch et al., 1994), but similar patterns were also observed using confocal microscopy (Fig. 3; supplementary material Movie 1). Note that although regions of high ratio values indicate areas of enhanced GFP–wGBD binding to membrane-associated active Cdc42, GFP–wGBD fluorescence measurements also include the unbound diffusible pool of the fluorescent biosensor, which is most abundant in the axon and growth cone central domain. If GFP–wGBD localization was determined solely by diffusion, the GFP fluorescence signal should decrease toward the periphery of the growth cone, in a similar manner to TMR-D fluorescence, which represents a reduced volume. However, we found that GFP–wGBD fluorescence was often elevated in the peripheral domain of growth cones on laminin relative to the central domain (Fig. 3A), which is opposite to the pattern observed with TMR-D (Fig. 3B). An image ratio confirms peripheral enrichment of GFP–wGBD relative to TMR-D (Fig. 3C), indicating that active Cdc42 is enriched within lamellipodia and filopodia where it might function to promote actin polymerization at the growth cone leading edge. By contrast, control growth cones expressing unconjugated GFP and TMR-D did not exhibit significant enrichment of GFP at their periphery (data not shown).

To confirm the specificity of our Cdc42 biosensor, we imaged growth cones during acute application of a cell-permeable Cdc42-specific inhibitory peptide containing the Cdc42- and Rac1-binding (CRIB) domain of N-WASP fused to the antennepedia internalization sequence and biotinylated at the N-terminus (Västrik et al., 1999). The CRIB peptide competes with GFP–wGBD for binding of active Cdc42, such that excess peptide should displace GFP–wGBD and disrupt its peripheral enrichment. Using TMR–steptavidin labeling, we found that the CRIB peptide was internalized within growth cones after a 1 minute treatment (supplementary material Fig. S3). Addition of the CRIB peptide rapidly homogenized GFP–wGBD distribution relative to TMR-D and led to lamellar retraction (Fig. 3D–F; supplementary material Movie 1), whereas addition of control medium had no effect (data not shown). Quantification of wGBD to TMR ratio values within the growth cone central and peripheral domains, as well as in the axon, confirmed that GFP–wGBD was specifically enriched at the peripheral domain and that this enrichment was significantly reduced by application of the CRIB peptide (Fig. 3E). A single-line kymograph constructed from the leading edge of a GFP–wGBD- and TMR-D-labeled growth cone before Cdc42 inhibition confirmed that extending lamellipodia contained enriched levels of GFP–wGBD (Fig. 3F). However, within 3 minutes of CRIB peptide addition, the peripheral GFP–wGBD enrichment was completely abolished and lamellipodial motility ceased. We also tested the effects of SecramineA (SecA), a small molecule Cdc42 inhibitor that functions in a RhoGDI-dependent manner (Pelish et al., 2006). This inhibitor functions differently to the CRIB peptide, disrupting Cdc42 activation rather than binding of active Cdc42 by the GFP–wGBD biosensor. Application of 1 μM SecA resulted in an immediate drop in peripheral Cdc42 activity and strongly reduced protrusive activity (Fig. 3G,H). These findings validate the specificity and sensitivity of the GFP–wGBD biosensor to detect Cdc42 activity and indicate that Cdc42 activity at the growth cone leading edge regulates lamellipodial dynamics.

To examine the role of FAK in the regulation of Cdc42 activity in growth cones on laminin, we tested the effects of a novel and specific FAK inhibitor, PF-573,228 (PF-228) (Slack-Davis et al., 2007). PF-228 is an ATP analogue that specifically interacts with FAK (IC_{50} of 4 nM), with a 250-times lower affinity to the

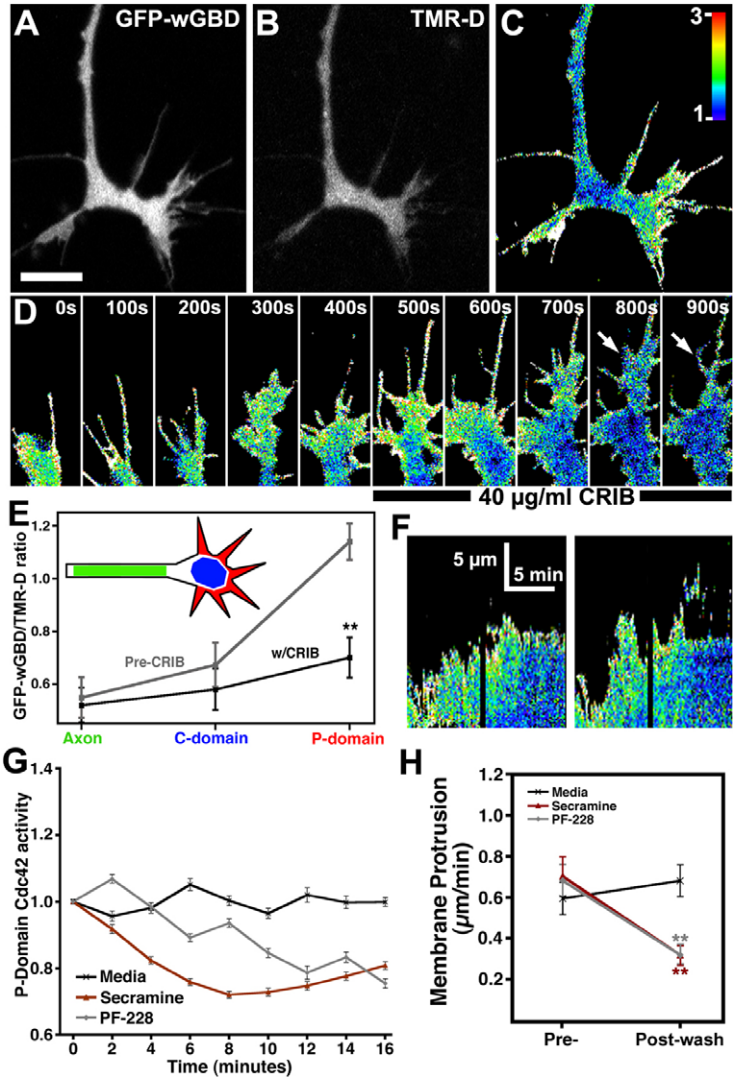

Fig. 3. Live imaging of Cdc42 activity in growth cones. (**A**,**B**) GFP–wGBD and TMR-D fluorescence images of a growth cone on LN. Note brighter leading edge fluorescence intensity of GFP–wGDB signal relative to TMR-D. (**C**) A pseudocolored ratio image of the growth cone in A and B shows the GFP–wGBD:TMR-D ratio is elevated throughout peripheral lamellipodia and filopodia. (**D**) Ratio images of the growth cone in C at the indicated times during exposure to 40 µg/ml N-WASP CRIB-peptide (at 450 seconds). Note reduced ratio at the periphery prior to lamellipodial retraction (arrows). (**E**) Quantification of GFP–wGBD:TMR-D fluorescence ratio measurements in the regions indicated in the schematic drawing (axon, C-domain and P-domain) before and 3 minutes after inhibition of Cdc42 with the CRIB peptide. High Cdc42 activity in the P-domain is significantly reduced compared with that for the C-domain and axon, where baseline Cdc42 activity is low. (**F**) Single line kymographs constructed from two protrusive regions of growth cone (C). Note an elevated wGBD:TMR-D ratio during lamellipodial protrusion before CRIB peptide addition, followed by a reduced ratio and cessation of lamellipodial dynamics after CRIB peptide addition. (**G**) Timecourse of peripheral domain Cdc42 activity during application of the Cdc42 inhibitor SecA, or the FAK inhibitor PF-228. Both treatments give significantly different results from those with control media (as determined by 2-way ANOVA; $n=14$ growth cones for media and PF-228, $n=18$ for SecA). (**H**) The effects of SecA and PF-228 on total membrane protrusion in wild-type TMR-D-loaded growth cones. The extent of protrusion was analyzed for 10 minutes before and 10 minutes following inhibitor addition. $^{**}P<0.001$, $n=10$ for growth cones in E, $n\geq14$ growth cones for G,H (as determined by Student's *t*-test). Scale bar: 10 µm or as indicated in kymographs.

closely related FAK homologue, Pyk2 (IC_{50} of 1000 nM). PF-228 was used at 100 nM, which dephosphorylates FAK at Y397, but does not cause collapse or retraction of axons (data not shown). Acute inhibition of FAK with PF-228 resulted in a delayed decrease in Cdc42 activity, which began around 6 minutes after treatment and was comparable to levels obtained with SecA by 12 minutes. Additionally, PF-228 resulted in a very similar decrease in membrane protrusion (Fig. 3G). The slower kinetics of FAK inhibition versus direct inhibition in reducing Cdc42 levels might be due to activated intermediate FAK effectors, such as p130Cas and DOCK180, which eventually cannot be maintained without active FAK. This result provides evidence that FAK is essential to the maintenance of Cdc42 activity in growth cones.

Cdc42 activity correlates with lamellipodial and filopodial protrusion

Studies examining fibroblast motility have demonstrated that active Cdc42 is enriched within protrusive lamellipodia at the cell periphery (Nalbant et al., 2004). To confirm these findings in neuronal growth cones, we compared GFP–wGBD to TMR-D ratio levels in lamellipodia during periods of extension and retraction. We found that elevated Cdc42 activity correlated with periods of lamellipodial extension, whereas reduced Cdc42 activity correlated with periods of retraction (Fig. 4A–C). To analyze Cdc42 activity in relation to lamellipodial extension, we constructed single-line kymographs from active regions of growth cones expressing GFP–wGBD and TMR-D. Kymographs were then used to measure the GFP–wGBD to TMR-D ratio at the distal 3 µm of the leading edge during both extension and retraction events. This analysis confirmed that lamellipodial retraction events coincided with a significant reduction in Cdc42 activity compared with extension events (Fig. 4C).

Cdc42 has also been implicated in the regulation of filopodial extension in many cell types (Nobes and Hall, 1995; Krugmann et al., 2001; Peng et al., 2003). For example, our previous studies implicated Cdc42 and its effector p21-activated kinase (PAK) in the regulation of filopodial motility in growth cones (Robles et al., 2005). To determine whether active Cdc42 also coincides with extending filopodia, we measured Cdc42 activity at the tips of filopodia (distal 1 µm region of filopodia). This analysis revealed that Cdc42 activity was highest at the tips of filopodia during extension compared with levels during retraction (Fig. 4F). In

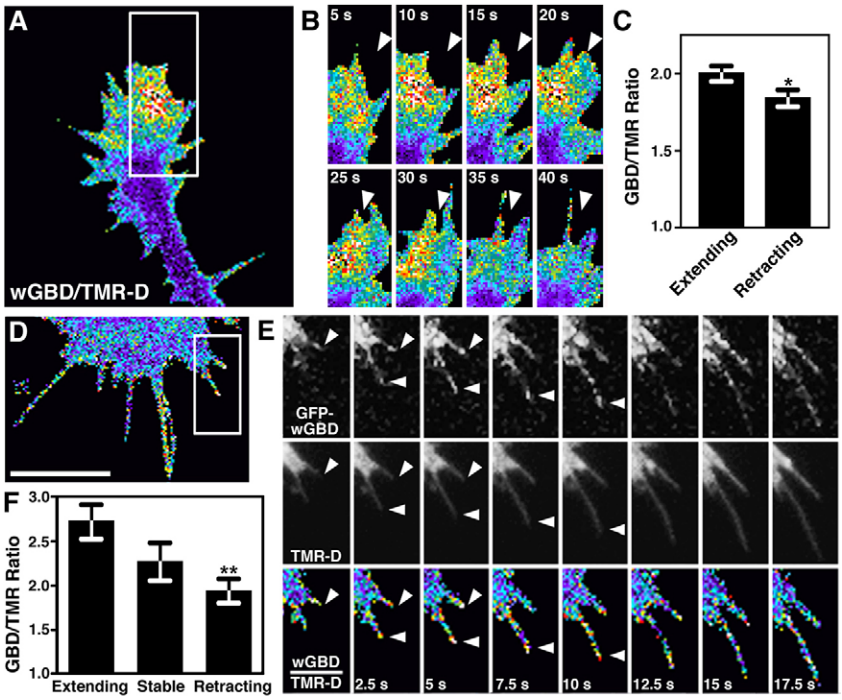

Fig. 4. Cdc42 activity is elevated at sites of filopodial and lamellipodial protrusion. (**A**) GFP–wGBD to TMR-D ratio image of a growth cone on laminin. (**B**) Time-lapse images at 5 second intervals of boxed region in A during extension (top row) and retraction (bottom row) of lamellipodia. Note elevated ratio during extension and subsequent decrease during lamellipodial retraction (arrowheads). (**C**) Quantification of GFP–wGBD to TMR-D ratio at the leading edge (3–4 μm region) of extending and retracting lamellipodia. Correlations were made using single-line kymographs of ratio image sequence. $n=40$ lamellipodia. (**D**) GFP–wGBD to TMR-D ratio image of a growth cone on laminin. (**E**) Time-lapse images at 2.5 second intervals of GFP–wGBD (top), TMR-D fluorescence (middle) and ratio images (bottom) of boxed region in D during extension of two filopodia. Note brief enrichment of GFP–wGBD at the tips of filopodia during extension (arrowheads). (**F**) Quantification of GFP–wGBD to TMR-D ratio at the distal tip (1 μm region) of filopodia during extension, stabilization and retraction. Only filopodia that exhibited periods of extension and retraction during the image sequence were analyzed. $n=40$ filopodia. $^{**}P<0.05$, $^{*}P<0.01$ using Student's *t*-test. Scale bars: 10 μm (A), 3 μm (D).

some instances, GFP–wGBD puncta were clearly visible at the tips of filopodia (Fig. 4E). However, it should be noted that these robust GFP–wGBD enrichments at the tips of filopodia were transient and not clearly detectable in all extending filopodia. Although these findings indicate that Cdc42 activity correlates with the generation of growth cone protrusions, it is likely that additional mechanisms also regulate the activity of Cdc42 effectors. For example, N-WASP activity can be modulated by PIP2 binding (Rohatgi et al., 2000) as well as phosphorylation by Src family kinases (Torres and Rosen, 2003).

Axon guidance cues rapidly modulate Cdc42 activity at the growth cone periphery

To determine the spatial and temporal dynamics of active Cdc42 in growth cones in response to positive and negative guidance cues, we examined the acute effects of BDNF, laminin and *Xenopus* Slit on GFP–wGBD- and TMR-D-labeled growth cones. BDNF and laminin stimulation typically led to a rapid and robust increase in the wGBD to TMR ratio at the growth cone periphery and subsequent lamellipodial ruffling and filopodial extension (Fig. 5, Fig. 6H; supplementary material Movies 2, 3). On average, Cdc42 activity within the growth cone peripheral domain peaked 360 seconds after BDNF or laminin addition (Fig. 6H), which correlates closely to the time course of activation reported in cerebellar granule cell neurons using a Cdc42 pull-down assay (Yuan et al., 2003). Importantly, activation of Cdc42 preceded BDNF and laminin-induced morphological changes, indicating that GFP–wGBD enrichment was not an artifact of movement or volume changes. The fact that BDNF and laminin stimulated motility in both GFP–wGBD-expressing and wild-type growth cones suggests that Cdc42 is interacting with endogenous functional targets in addition to the introduced Cdc42 biosensor. To control for possible non-specific effects, we confirmed that BDNF stimulation had no effect on the distribution of unconjugated GFP in growth cones co-loaded with TMR-D (data not shown). In addition, we also showed similar changes in neurons co-expressing GFP–wGBD and mCherry–CAAX (supplementary material Fig. S4). Because mCherry–CAAX also targets the membrane, this result shows the GFP–wGBD is selectively enriched at the growth cone periphery in response to BDNF.

In contrast to BDNF and laminin stimulation, application of *Xenopus* Slit resulted in a complete loss of GFP–wGBD enrichment within the lamellipodia and filopodia of growth cones (Fig. 6A–F; supplementary material Movie 4). Reduced Cdc42 activity across the growth cone was similar to the effects of the CRIB peptide, SecA and PF-228 (Fig. 3H). Interestingly, the loss of GFP–wGBD enrichment at the periphery after addition of murine Slit2 was slow on average, reaching a minimum ratio of 0.65 ± 0.02 after 16 minutes ($n=12$ growth cones; Fig. 6H), which most closely resembled inhibition of FAK with PF-228. This reduction in Cdc42 activity coincided with a complete cessation of lamellipodial and filopodial motility. These findings confirm that positive and negative guidance cues rapidly modulate Cdc42 activity at the growth cone periphery.

FAK is necessary for laminin- and BDNF-driven increases in Cdc42 activity

Previous work from our lab showed that FAK functions downstream of BDNF and laminin (Robles and Gomez, 2006; Myers and Gomez, 2011). To test the possibility that regulation of Cdc42 activity by BDNF and laminin requires FAK function, we expressed FRNK (FAK-related non-kinase) (Schaller et al., 1993), a dominant-negative FAK isoform, along with GFP–wGBD and TMR-D labeling. Strikingly, FRNK-expressing neurons showed no increase in peripheral Cdc42 activity on stimulation with BDNF (Fig. 7A,B,I). Moreover, application of laminin to FRNK-expressing neurons resulted in a modest decrease in Cdc42 activity (Fig. 7C,D,I; supplementary material Movie 4). This decrease in the ratio was maintained,

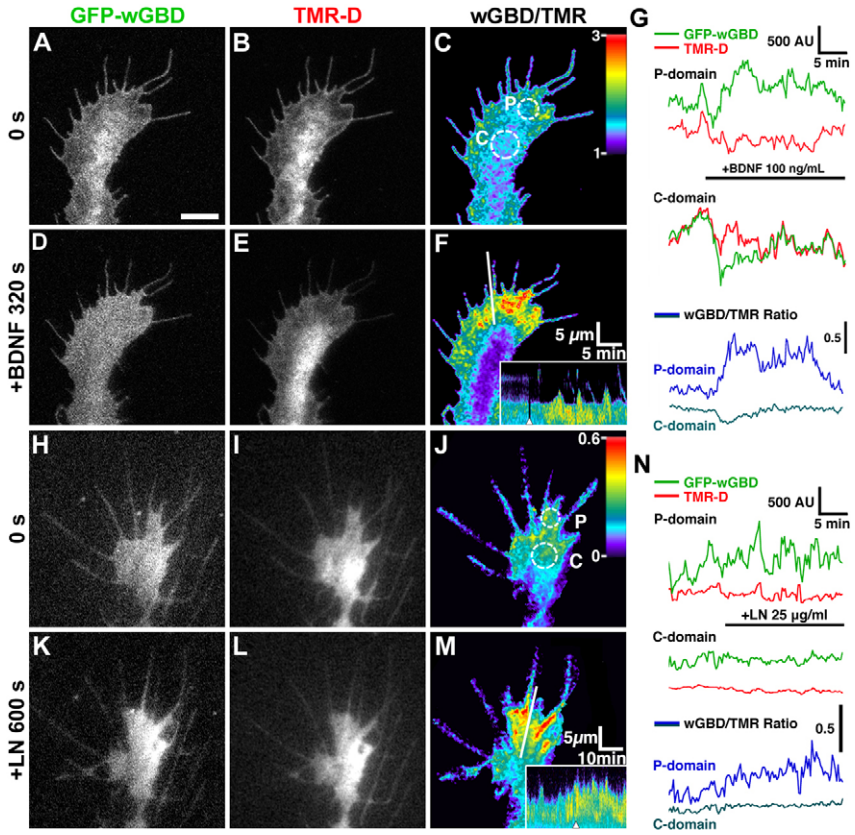

Fig. 5. BDNF and laminin activate Cdc42 at the growth cone periphery. (**A**,**B**) GFP–wGBD and TMR-D single-channel fluorescence confocal images of a growth cone on PDL before BDNF stimulation. (**C**) GFP–wGBD to TMR-D ratio image of growth cone in A and B. (**D–F**) Single-channel and fluorescence ratio images 320 seconds following BDNF application. Note a robust increase in the wGBD to TMR-D ratio is apparent at the growth cone periphery by 320 seconds following stimulation. Increased peripheral wGBD to TMR-D ratio is due to apparent movement of GFP–wGBD from central domain to the periphery (compare A and D). Inset in F shows a single-line kymograph constructed from region indicated by the white line in F. Note an elevated wGBD to TMR-D ratio during lamellipodial protrusion. (**G**) Fluorescence intensity measurements (12-bit scale) over time within regions indicated in C. Top and middle traces: GFP–wGBD and TMR-D fluorescence intensities within the peripheral (P) and central (C) regions, respectively. Lower trace: GFP–wGBD to TMR-D ratio measurements in the P and C domains. Increased ratio at the growth cone periphery suggests that BDNF locally activates Cdc42. Slight drop in C-domain ratio following BDNF stimulation is probably due to reduced cytosolic pool of GFP–wGBD upon recruitment to membrane-associated active Cdc42 (see A and D). (**H–M**) As in A–F, single channel and ratio images of a growth immediately before (H–J) and 600 seconds after laminin application (K–M). Note the increased ratio in the peripheral domain and the higher ratio at the base of filopodia. Inset in M shows a single-line kymograph constructed from region indicated by the white line in M. Note the elevated wGBD to TMR-D ratio during lamellipodial protrusion. (**N**) Similar fluorescent intensity analysis as described in G for neuron in H–M. Pseudocolor scale in C applies to C,F, that in J to J,M. Scale bar: 5 μm or as indicated for the kymographs.

indicating that this is a sustained loss of Cdc42 activity. This suggests that laminin, unlike BDNF, promotes FAK-independent inhibition of Cdc42, as well as a FAK-dependent activation of Cdc42. FRNK-expressing neurons showed lower basal protrusions relative to wild-type, which did not increase with application of BDNF (Fig. 7J). Laminin application resulted in a modest, but significant decrease in protrusion by FRNK neurons, again indicating that Cdc42 activity is inhibited on laminin stimulation.

To support the role for FAK upstream of Cdc42, we tested the effects of treatment with the small molecule FAK inhibitor PF-228. Unlike control neurons, simultaneous application of PF-228 with BDNF or laminin on wild-type neurons expressing GFP–wGBD did not result in a significant increase in Cdc42 activity (Fig. 7E–H,K). Interestingly, PF-228 and laminin together resulted in a modest decrease in Cdc42 activity, which is consistent with observations made with FRNK-expressing neurons (Fig. 7I). Protrusive activity showed a similarly sharp decrease with PF-228 and BDNF or laminin application (Fig. 7L).

Constitutively active FAK prevents Slit2 inhibition of Cdc42

To determine whether inactivation of FAK is necessary for Slit2-mediated inhibition of Cdc42 activity and membrane protrusion, we expressed SuperFAK along with GFP–wGBD and TMR-D labeling. Unlike control neurons, SuperFAK-expressing neurons exhibited little change in Cdc42 activity after stimulation with 250 ng/ml Slit2 (Fig. 8A–C; supplementary material Movie 5). Protrusion analysis by kymograph revealed that SuperFAK neurons are less protrusive than wild-type neurons at baseline (Fig. 1I), but that Slit2 stimulation does not further decrease protrusion by these growth cones. The reduced number of basal protrusions in SuperFAK neurons suggests that balanced FAK activity is necessary for optimal cell motility. Indeed, we found that the rate of axon outgrowth by SuperFAK-expressing neurons is slower than wild-type neurons [SuperFAK 34.7±2.4 (n=56)

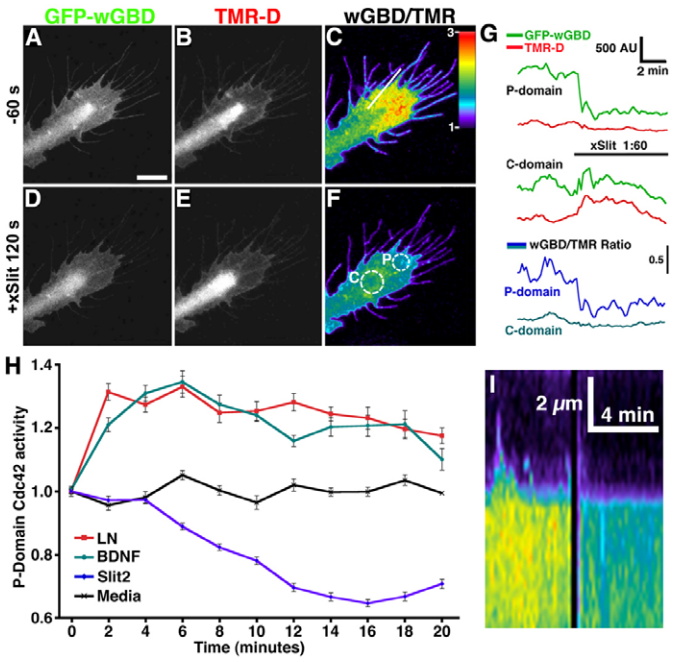

Fig. 6. Slit disrupts enrichment of Cdc42 at the growth cone periphery. (**A–F**) Single channel (GFP–wGBD and TMR-D) and fluorescence ratio images before (A–C) and 120 seconds following *Xenopus* Slit application (D–E). Note decreased GFP–wGBD to TMR-D ratio at the growth cone periphery is due to rearward movement of GFP–wGBD from peripheral domain to the central region (compare A and D). (**G**) Fluorescence intensity measurements (12-bit scale) over time within regions indicated in F. Top and middle traces: GFP–wGBD and TMR-D fluorescence intensities within the peripheral (P) and central (C) regions, respectively. Bottom trace: GFP–wGBD to TMR-D ratio measurements in P and C domains. Pseudocolor scale in C applies to C and F. Scale bar: 5 μm. (**H**) Time course of peripheral Cdc42 activity in growth cones in response to control medium or medium containing 100 ng/ml BDNF, 25 μg/ml laminin or 250 ng/ml Slit2. Cdc42 is significantly elevated at all time points after laminin and BDNF addition and significantly reduced after 4 minutes of Slit2 addition compared with control medium by two-way ANOVA. $n \geq 14$ growth cones for each condition. (**I**) A single line kymograph constructed from the region indicated by the white line in C. Note that both the wGBD/TMR-D ratio and lamellipodial protrusions are reduced after xSlit application.

and WT was 43.2±1.3 ($n=60$) and similar to FRNK-expressing neurons (Myers and Gomez, 2011)]. Together, these data support a model of common regulation of Cdc42 by BDNF, laminin and Slit2 through modulation of FAK activity, potentially through an effector such as p130Cas.

Discussion

In this study we quantify for the first time the spatial and temporal dynamics of Cdc42 activity in spinal neuron growth cones in response to physiologically relevant axon guidance factors. We show that changes in Cdc42 activity are required for the growth-promoting effects of laminin and BDNF and the inhibitory actions of Slit on *Xenopus* spinal neuron growth cone motility. In addition, we identify FAK as a necessary upstream modulator of Cdc42 in response to BDNF, laminin and Slit. Using a fluorescent Cdc42 biosensor, we show that local elevations in Cdc42 activity correlate with protrusive behaviors of both lamellipodia and filopodia. This biosensor permitted direct visualization of rapid laminin-, BDNF- and Slit-induced modulation of Cdc42 activity at the growth cone periphery. Molecular and pharmacological inhibition of FAK prevented Cdc42 activation by BDNF and laminin, whereas constitutively active FAK blocked the Slit-mediated decrease in Cdc42 activity. Together, these findings suggest that rapid modulation of Cdc42 signaling at the growth cone leading edge controls lamellipodial and filopodial dynamics downstream of guidance cue receptors through corresponding changes in FAK activity.

Cdc42 has been implicated as a necessary signaling component for normal brain development (Garvalov et al., 2007) downstream of growth factors and guidance cues. For example, biochemical pull-down assays revealed that the chemoattractants Netrin and BDNF elevate levels of active Cdc42 in developing neurons (Jin et al., 2005; Shekarabi et al., 2005). Activation of Cdc42 in these studies correlated with altered growth cone morphologies and increased motility. Conversely, the chemorepellant Slit reduces Cdc42 activity (Wong et al., 2001), which leads to growth cone collapse in vitro (Nguyen Ba-Charvet et al., 1999). Our findings show that the acute effects of laminin, BDNF and Slit on growth cone motility result from rapid modulation of Cdc42 activity at the growth cone periphery through FAK. This is the first demonstration of the spatial and temporal dynamics of Cdc42 activation in growth cones stimulated by established axon guidance cues. Our findings are consistent with a model where rapid and local modulation of GTPase activity underlies growth cone pathfinding behaviors made in response to guidance cues within decision regions. Numerous upstream GEFs and GAPs for Cdc42 are enriched in growth cones (Pertz et. al., 2008), which probably controls the diverse combinatorial effects growth factors and ECM molecules have on axon pathfinding.

Imaging Cdc42 activity in live neurons also allowed us to directly compare growth cone motility with levels of active Cdc42. We found that the protrusion of both filopodia and lamellipodia correlated with increased levels of active Cdc42 within these subcellular domains. This result suggests that Cdc42 activation at the growth cone periphery activates domain-specific effector molecules to control distinct cellular behaviors. For example, our previous work demonstrated that the Cdc42 effector PAK is specifically recruited to the tips of filopodia and functions to regulate filopodial motility (Robles et al., 2005). Our current findings suggest that specific Cdc42 effectors also regulate lamellipodial motility. One potential candidate is N-WASP, which activates Arp2/3-dependent actin polymerization to form branched arrays of filamentous actin (reviewed by Welch, 1999). Consistent with this possibility, studies using fluorescence resonance energy transfer (FRET) probes have detected enriched levels of active Cdc42 and N-WASP in motile lamellipodia at the periphery of migratory non-neuronal cells (Kurokawa et al., 2004; Lorenz et al., 2004; Nalbant et al., 2004; Ward et al., 2004). However, more recent work in fibroblasts suggests that active Cdc42 is not precisely associated in space and time with the distal edge of protrusions (Machacek et al., 2009). This might reflect the difference between non-neuronal cells and growth cones because previous studies of growth cones using FRET-based biosensors (Nakamura et al., 2005) reported similar distributions to those described here. It is also noteworthy that growth cone protrusions not only had elevated levels of active Cdc42 relative to non-protrusive regions (Figs 3, 4), but that levels often fluctuated dramatically as individual protrusions

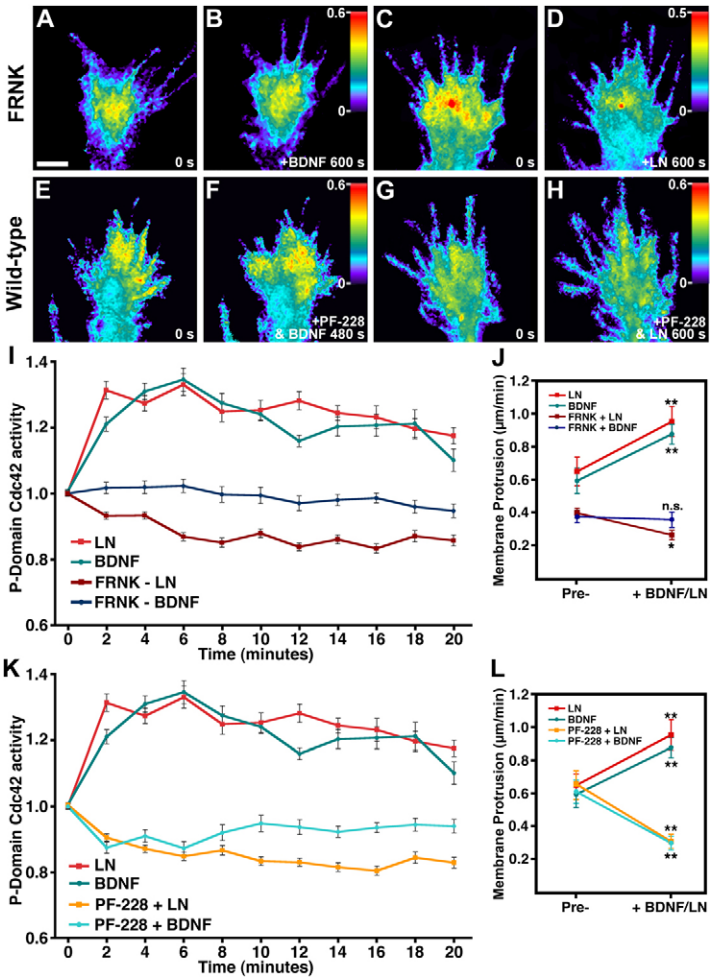

Fig. 7. BDNF and laminin require FAK to modulate Cdc42 activity and protrusion. (**A–D**) Fluorescence ratio images of GFP–wGBD and TMR-D before (A,C) and 600 seconds after BDNF or laminin application (B,D) in FRNK-expressing growth cones. Note that Cdc42 activity does not change at the growth periphery following BDNF and is slightly reduced following laminin application. Single-channel (GFP–wGBD and TMR-D) fluorescence images are shown in supplementary material Fig. S5. (**E–H**) Fluorescence ratio images of GFP–wGBD and TMR-D before (E,G) and 480 or 600 seconds following simultaneous addition of 100 nM PF-228 and BDNF or laminin (F,H). Note that Cdc42 activity does not change at the growth periphery in the presence of PF-228 and BDNF or laminin application. Single-channel (GFP–wGBD and TMR-D) fluorescence images are shown in supplementary material Fig. S6. (**I**) Time course of peripheral Cdc42 activity in growth cones in response to BDNF or laminin in control or FRNK-expressing growth cones. Note the sustained decrease in Cdc42 activity on laminin application in FRNK-expressing neurons. $n \geq 14$ growth cones for each condition. (**J**) Changes in leading edge protrusion 10 minutes before and 10 minutes after BDNF or laminin application in control or FRNK-expressing growth cones. Note reduced basal protrusive activity in FRNK neurons and further decrease on laminin application. $n \geq 20$ growth cones for each condition. (**K**) Time course of peripheral Cdc42 activity in growth cones in response to BDNF or laminin with or without simultaneous application of PF-228. Note decreased Cdc42 activity on laminin application. $n \geq 14$ growth cones for each condition. (**L**) Changes in leading edge protrusion 10 minutes before and 10 minutes after BDNF or laminin application with or without simultaneous application of PF-228. Note that data from both P-domain Cdc42 activity (I,K) and protrusion (J,L) of wild-type BDNF and laminin responses were replicated for comparison from supplementary material Figs S1, S6. FRNK+LN is significantly less than control medium after 4 minutes by two-way ANOVA (I). Cdc42 is significantly reduced at 6 and 18 minutes after PF-228+BDNF addition and at all time points after 2 minutes PF-228+LN addition compared with control medium by two-way ANOVA. $n \geq 20$ growth cones for each condition. $^{**}P<0.01$, $^{*}P<0.05$. Scale bar: 5 μm.

underwent cycles of extension and retraction. Although there was no apparent link between fluctuations in Cdc42 activity and membrane protrusion, it is possible that our temporal and spatial resolution is not high enough to make this correlation.

Focal adhesion kinase is known to regulate several Rho GTPases and function downstream of a number of axon guidance cues, making it a compelling signal integrator within growth cones. One of the first identified effectors of FAK is GTPase regulator associated with FAK (GRAF), which is a RhoA/Cdc42 GTPase activating protein (GAP) (Hildebrand et al., 1996). Additionally, FAK is known to bind and activate both p190RhoGEF and p190RhoGAP, which have opposite effects on RhoA activity. FAK-null fibroblasts display an elevated level of RhoA activity (Ren et al., 2000) that might be due to reduced p190RhoGAP activation, which is activated on integrin engagement (Arthur et al., 2000). By contrast, FAK can activate RhoA in some contexts through p190RhoGEF, which regulates axon branching and synapse formation (Rico et al., 2004). In addition to Cdc42 inactivation through GRAF, FAK might also activate Cdc42 signaling. FAK is phosphorylated at Y861 by Src, and this creates a binding site for the scaffolding protein p130Cas (Cho and Klemke, 2002). Subsequently, p130Cas associates with the Rac GEF DOCK180, which leads to Rac activation downstream of integrin engagement (Brugnera et al., 2002; Côté and Vuori, 2002). Interestingly, p130Cas was found to activate both Rac1 and Cdc42 downstream of Netrin signaling, which is necessary for midline crossing by commissural interneurons (Liu et al., 2007). Therefore, it appears that FAK is capable of activating or inactivating both RhoA and Cdc42, depending on the particular GEF or GAP protein involved. In support of this notion is the identification of DOCK180 homologues that interact with p130Cas and activate both Rac1 and Cdc42 (Côté and Vuori, 2002). The data we present here suggest that changes in FAK activity modulate a Cdc42 GEF, such as DOCK180, to control Cdc42 function. Although repulsive guidance cues such as Slit2 might also inhibit Cdc42 by activating the Cdc42 GAP srGAP1 (Wong et al., 2001), our results suggest this does not occur in the presence of constitutively active SuperFAK.

This study demonstrated rapid and local activation and inactivation of Cdc42 through corresponding modulation of FAK in growth cones acutely stimulated with positive and negative guidance cues, respectively. FAK activation has been linked to a variety of guidance cues, including Netrin (Li et al., 2004; Liu et al., 2004; Ren et al., 2004), BDNF (Fig. 2) (Myers and Gomez, 2011), Sema3A (Bechara et al., 2008), Ephs and Ephrins (Woo et al., 2009), and MAG (myelin-associated glycoprotein) (Goh et al., 2008). FAK dephosphorylation at Y397 has been linked to RGM (repulsive guidance molecule) (Endo and Yamashita, 2009) and the work presented here links Slit2 repulsion to FAK inactivation by dephosphorylation at both Y397 and Y861. These results place FAK as a general signal

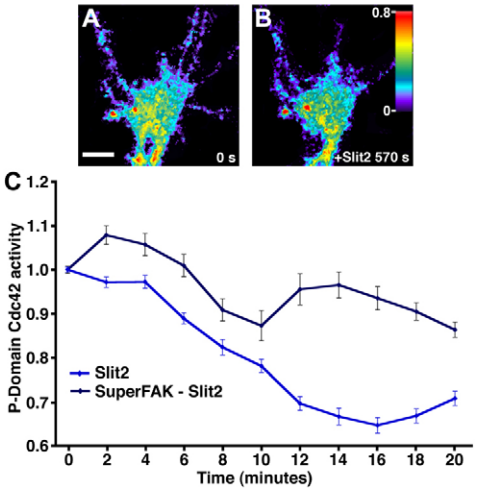

Fig. 8. Slit2 inhibition of Cdc42 is blocked by constitutively active FAK. (**A**,**B**) Fluorescence ratio images of GFP–wGBD and TMR-D before (A) and 570 seconds after Slit2 application (B) in a SuperFAK-expressing growth cone. Single-channel (GFP–wGBD and TMR-D) fluorescence images are shown in supplementary material Fig. S7. (**C**) Average change in Cdc42 activity over time at the growth cone periphery in response to Slit2 in control or SuperFAK expressing growth cones. Note less change Cdc42 activity in SuperFAK-expressing neurons. Control Slit2 response from Fig. 6 is presented again for comparison. Cdc42 activity becomes significantly ($P<0.01$) different between SuperFAK and control neurons 12 minutes after treatment with Slit2. $n=14$ growth cones for each condition. Scale bar: 5 μm.

integrator downstream of diverse axon guidance cues and indicate that FAK control of growth cone motility proceeds through Rho family GTPases. Because FAK can be activated by both positive and negative cues, it will be interesting to test how Cdc42 activity is modulated in response to inhibitory cues known to activate FAK. Under such conditions, FAK signaling might be directed toward GEFs that preferentially activate RhoA over Cdc42. Alternatively, Cdc42 might also be activated by inhibitory cues, but these signals could be overridden by stronger inhibitory signals in parallel. Fluorescent reporters of RhoA, Rac1 and Cdc42 activity make it possible to test the activation of each of these GTPases during stimulation with positive and negative guidance cues. Future work using these biosensors, together with pharmacological agents and axon guidance cues, should provide additional molecular insights into cellular mechanisms controlling the formation of neural circuits in the developing nervous system.

Materials and Methods

Embryo injection and cell culture

All expression constructs were subcloned into the pCS2+ vector for RNA synthesis (Dave Turner, University of Michigan, Ann Arbor, MI), with either a GFP or Myc tag. Human isoforms of mutant Cdc42 constructs (Q61L constitutively active and T17N dominant negative) in pCS2+ were provided by Alan Hall (Sloan-Kettering Institute, New York, NY). GFP–wGBD and mCherry-CAAX plasmids were provided by Bill Bement (University of Wisconsin, Madison, WI). GFP–FRNK was provided by Patti Keely (University of Wisconsin). SuperFAK was provided by Michael Schaller (West Virginia University, Morgantown, WV). Two blastomeres at the eight-cell-stage of *Xenopus laevis* embryos were injected with capped mRNA transcribed in vitro (mMessage machine, Ambion, Foster City, CA). For DNCdc42, GFP, GFP–wGBD, Myc–FRNK or Myc–SuperFAK 0.3 ng/blastomere mRNA was injected. A maximum of 0.1 ng CA-Cdc42 mRNA was injected to allow embryo survival and normal development. For dual-labeling experiments, embryos were co-injected with 50–100 ng of tetramethylrhodamine–dextran (TMR-D, 10,000 MW; Invitrogen, Carlsbad, CA) and mRNA. Neural tubes were dissected from stage 24 or stage 28 *Xenopus* embryos and cultured as previously described (Gómez et al., 2003). Neural tube explants were plated onto acid-washed coverslips coated with 50 μg/ml PDL (Sigma, St Louis, MO) or 25 μg/ml laminin (Sigma) and imaged or fixed 16–24 hours following plating.

Reagents and immunostaining

BDNF (Promega, Madison, WI) was applied at 100 ng/ml. *Xenopus* Slit-conditioned medium was obtained from stably transfected HEK cells generously provided by Yi Rao (National Institute of Biological Sciences, Beijing, China). This medium was concentrated using a Biomax-100 filtration device (Millipore, Billerica, MA) and applied at a 1:100 dilution. Slit2 (R&D systems, Minneapolis, MN) was applied at 250 ng/ml unless otherwise noted. Laminin (Sigma) was applied at 25 μg/ml. PF-557,228 (Tocris, Ellisville, MO) was applied at 100 nM. SecramineA was a gift from Tom Kirchhausen (Harvard Medical School, Cambridge, MA). For immunocytochemistry, cultures were fixed in 4% paraformaldehyde in Krebs + sucrose fixative (4% PKS) (Dent and Meiri, 1992) and permeabilized with 0.1% Triton X-100 in CMF-PBS. Alexa Fluor 546 phalloidin (Invitrogen) was used to label filamentous actin (F-actin). Primary antibodies against tyrosine-phosphorylated FAK and Src (Invitrogen) were used at 1:500 in blocking solution. Alexa-Fluor-conjugated secondary antibodies were purchased from Invitrogen and used at 1:250 in blocking solution. The biotinylated N-WASP CRIB peptide was synthesized by the University of Wisconsin Peptide Synthesis Facility as described previously (Västrik et al., 1999) and internalization was confirmed by FITC–streptavidin staining.

Image acquisition and analysis

For both live and fixed fluorescent microscopy, high-magnification images were acquired using either a 60× /1.45 NA objective lens on an Olympus Fluoview 500 laser-scanning confocal system mounted on an AX-70 upright microscope or a 100× /1.49 NA objective lens on a Nikon total internal reflection fluorescence (TIRF) microscope using an EVOLVE 512 EMCCD camera (Photometrics, Tucson, AZ). Growth cones were imaged at 2–2.5× zoom (pixel size, 165–200 nm). GFP–wGBD and TMR-D was excited sequentially with 488 nm and 543 laser lines of the confocal and 488 nm and 563 nm laser lines of the TIRF microscope. For bright-field time-lapse microscopy, low-magnification phase-contrast images were acquired using a 20× objective on a Nikon microscope equipped with an *x–y* motorized stage for multi-positional imaging. Live explant cultures were sealed in enclosed perfusion chambers as described previously (Gómez et al., 2003) to allow rapid exchange of solutions. Images were analyzed using ImageJ software (National Institutes of Health, Bethesda, MD). Measurements of tyrosine-phosphorylated FAK and Src immunolabeled images were made by first selecting the perimeter of growth cones from thresholded F-actin-labeled images based on intensity to exclude background as described (Woo et al., 2009). These user-defined regions were then used to measure the average pixel intensity of phosphorylated tyrosine labeling within non-thresholded growth cones. Background labeling was subtracted from these measured values and normalized to vehicle treated control growth cones. For display purposes, fluorescent images were scaled and pseudocolored using ImageJ look-up tables.

Membrane protrusion analysis

For membrane protrusion analysis, 1- to 2-pixel-wide kymographs were constructed using Metamorph software (Molecular Devices, Sunnyvale, CA) or ImageJ from lines spanning 3–4 distinct lamellipodial regions (typically between filopodial protrusions) at the periphery of each growth cone. For data analysis, the single most active growth cone region from each observation interval (pre- and post-treatment) was quantified to exclude the possibility that changes in protrusion reflected a localized change in the dynamics of an individual growth cone region. To reflect changes in both the size and frequency of protrusive events, the cumulative extent of protrusion in each growth cone region was summed and expressed as a function of interval duration. For BDNF or laminin treatments, membrane protrusion was quantified during time intervals 0–10 minutes before and 5–15 minutes following BDNF or laminin application. For *Xenopus* Slit and Slit2 experiments, membrane protrusion was quantified for 0–10 minutes before and 2–12 minutes following application of *Xenopus* Slit or Slit2. 100 nM PF-228 was applied simultaneously with BDNF or laminin. For growth cone area measurements, the distal 10 μm segment of each axon was analyzed using Metamorph software.

Cdc42 activity analysis

Ratiometric images were constructed from single-channel GFP–wGBD and TMR-D image stacks using Metafluor software (Molecular Devices) or ImageJ. For correlation analysis of Cdc42 activity and lamellipodial dynamics, 1- or 2-line kymographs were constructed from ratio image sequences and ratio values were quantified from the distal 3 μm of the leading edge. Cdc42 activity within filopodia was measured from ratio values at the distal 1 μm segment of motile filopodia. Cdc42 activity within the peripheral and central domains of growth cones were measured from user defined regions of at least 100 pixels.

Quantification was performed from images obtained by confocal and TIRF microscopy. Statistical significance was determined using Student's *t*-test, or two-way ANOVA with Bonferroni post-tests as specified in legends and variance is reported as ± s.e.m.

Acknowledgements

We thank Bill Bement, Erik Dent and members of the Gomez lab for comments on the manuscript.

Funding

This work was supported by the National Institutes of Health [grant number NS41564 to T.M.G.]. Deposited in PMC for release after 12 months.

Supplementary material available online at
http://jcs.biologists.org/lookup/suppl/doi:10.1242/jcs.100107/-/DC1

References

Arthur, W. T., Petch, L. A. and Burridge, K. (2000). Integrin engagement suppresses RhoA activity via a c-Src-dependent mechanism. *Curr. Biol.* **10**, 719-722.

Bechara, A., Nawabi, H., Moret, F., Yaron, A., Weaver, E., Bozon, M., Abouzid, K., Guan, J. L., Tessier-Lavigne, M., Lemmon, V. et al. (2008). FAK-MAPK-dependent adhesion disassembly downstream of L1 contributes to semaphorin3A-induced collapse. *EMBO J.* **27**, 1549-1562.

Bentley, D. and O'Connor, T. P. (1994). Cytoskeletal events in growth cone steering. *Curr. Opin. Neurobiol.* **4**, 43-48.

Bokoch, G. M., Bohl, B. P. and Chuang, T. H. (1994). Guanine nucleotide exchange regulates membrane translocation of Rac/Rho GTP-binding proteins. *J. Biol. Chem.* **269**, 31674-31679.

Brown, M. D., Cornejo, B. J., Kuhn, T. B. and Bamburg, J. R. (2000). Cdc42 stimulates neurite outgrowth and formation of growth cone filopodia and lamellipodia. *J. Neurobiol.* **43**, 352-364.

Brugnera, E., Haney, L., Grimsley, C., Lu, M., Walk, S. F., Tosello-Trampont, A. C., Macara, I. G., Madhani, H., Fink, G. R. and Ravichandran, K. S. (2002). Unconventional Rac-GEF activity is mediated through the Dock180-ELMO complex. *Nat. Cell Biol.* **4**, 574-582.

Cho, S. Y. and Klemke, R. L. (2002). Purification of pseudopodia from polarized cells reveals redistribution and activation of Rac through assembly of a CAS/Crk scaffold. *J. Cell Biol.* **156**, 725-736.

Côté, J. F. and Vuori, K. (2002). Identification of an evolutionarily conserved superfamily of DOCK180-related proteins with guanine nucleotide exchange activity. *J. Cell Sci.* **115**, 4901-4913.

Dent, E. W. and Meiri, K. F. (1992). GAP-43 phosphorylation is dynamically regulated in individual growth cones. *J. Neurobiol.* **23**, 1037-1053.

Dent, E. W. and Gertler, F. B. (2003). Cytoskeletal dynamics and transport in growth cone motility and axon guidance. *Neuron* **40**, 209-227.

Dent, E. W., Gupton, S. L. and Gertler, F. B. (2011). The growth cone cytoskeleton in axon outgrowth and guidance. *Cold Spring Harb. Perspect. Biol.* **3**, a001727.

Endo, M. and Yamashita, T. (2009). Inactivation of Ras by p120GAP via focal adhesion kinase dephosphorylation mediates RGMa-induced growth cone collapse. *J. Neurosci.* **29**, 6649-6662.

Fan, J. and Raper, J. A. (1995). Localized collapsing cues can steer growth cones without inducing their full collapse. *Neuron* **14**, 263-274.

Gabarra-Niecko, V., Keely, P. J. and Schaller, M. D. (2002). Characterization of an activated mutant of focal adhesion kinase: 'SuperFAK'. *Biochem. J.* **365**, 591-603.

Gallo, G. and Letourneau, P. C. (2004). Regulation of growth cone actin filaments by guidance cues. *J. Neurobiol.* **58**, 92-102.

Garvalov, B. K., Flynn, K. C., Neukirchen, D., Meyn, L., Teusch, N., Wu, X., Brakebusch, C., Bamburg, J. R. and Bradke, F. (2007). Cdc42 regulates cofilin during the establishment of neuronal polarity. *J. Neurosci.* **27**, 13117-13129.

Goh, E. L., Young, J. K., Kuwako, K., Tessier-Lavigne, M., He, Z., Griffin, J. W. and Ming, G. L. (2008). beta1-integrin mediates myelin-associated glycoprotein signaling in neuronal growth cones. *Mol. Brain* **1**, 10.

Gómez, T. M., Harrigan, D., Henley, J. and Robles, E. (2003). Working with Xenopus spinal neurons in live cell culture. *Methods Cell Biol.* **71**, 129-156.

Hildebrand, J. D., Taylor, J. M. and Parsons, J. T. (1996). An SH3 domain-containing GTPase-activating protein for Rho and Cdc42 associates with focal adhesion kinase. *Mol. Cell. Biol.* **16**, 3169-3178.

Hynes, R. O. (2002). Integrins: bidirectional, allosteric signaling machines. *Cell* **110**, 673-687.

Jin, M., Guan, C. B., Jiang, Y. A., Chen, G., Zhao, C. T., Cui, K., Song, Y. Q., Wu, C. P., Poo, M. M. and Yuan, X. B. (2005). Ca2+-dependent regulation of rho GTPases triggers turning of nerve growth cones. *J. Neurosci.* **25**, 2338-2347.

Kater, S. B. and Rehder, V. (1995). The sensory-motor role of growth cone filopodia. *Curr. Opin. Neurobiol.* **5**, 68-74.

Krugmann, S., Jordens, I., Gevaert, K., Driessens, M., Vandekerckhove, J. and Hall, A. (2001). Cdc42 induces filopodia by promoting the formation of an IRSp53:Mena complex. *Curr. Biol.* **11**, 1645-1655.

Kurokawa, K., Itoh, R. E., Yoshizaki, H., Nakamura, Y. O. and Matsuda, M. (2004). Coactivation of Rac1 and Cdc42 at lamellipodia and membrane ruffles induced by epidermal growth factor. *Mol. Biol. Cell* **15**, 1003-1010.

Li, W., Lee, J., Vikis, H. G., Lee, S. H., Liu, G., Aurandt, J., Shen, T. L., Fearon, E. R., Guan, J. L., Han, M. et al. (2004). Activation of FAK and Src are receptor-proximal events required for netrin signaling. *Nat. Neurosci.* **7**, 1213-1221.

Liu, G., Beggs, H., Jürgensen, C., Park, H. T., Tang, H., Gorski, J., Jones, K. R., Reichardt, L. F., Wu, J. and Rao, Y. (2004). Netrin requires focal adhesion kinase and Src family kinases for axon outgrowth and attraction. *Nat. Neurosci.* **7**, 1222-1232.

Liu, G., Li, W., Gao, X., Li, X., Jürgensen, C., Park, H. T., Shin, N. Y., Yu, J., He, M. L., Hanks, S. K. et al. (2007). p130CAS is required for netrin signaling and commissural axon guidance. *J. Neurosci.* **27**, 957-968.

Lorenz, M., Yamaguchi, H., Wang, Y., Singer, R. H. and Condeelis, J. (2004). Imaging sites of N-wasp activity in lamellipodia and invadopodia of carcinoma cells. *Curr. Biol.* **14**, 697-703.

Machacek, M., Hodgson, L., Welch, C., Elliott, H., Pertz, O., Nalbant, P., Abell, A., Johnson, G. L., Hahn, K. M. and Danuser, G. (2009). Coordination of Rho GTPase activities during cell protrusion. *Nature* **461**, 99-103.

Meyer, G. and Feldman, E. L. (2002). Signaling mechanisms that regulate actin-based motility processes in the nervous system. *J. Neurochem.* **83**, 490-503.

Mitra, S. K., Hanson, D. A. and Schlaepfer, D. D. (2005). Focal adhesion kinase: in command and control of cell motility. *Nat. Rev. Mol. Cell Biol.* **6**, 56-68.

Myers, J. P. and Gomez, T. M. (2011). Focal adhesion kinase promotes integrin adhesion dynamics necessary for chemotropic turning of nerve growth cones. *J. Neurosci.* **31**, 13585-13595.

Nakamura, T., Aoki, K and Matsuda, M. (2005). FRET imaging in nerve growth cones reveals a high level of RhoA activity within the peripheral domain. *Brain Res. Mol. Brain Res.* **139**, 277-287.

Nalbant, P., Hodgson, L., Kraynov, V., Toutchkine, A. and Hahn, K. M. (2004). Activation of endogenous Cdc42 visualized in living cells. *Science* **305**, 1615-1619.

Nguyen Ba-Charvet, K. T., Brose, K., Marillat, V., Kidd, T., Goodman, C. S., Tessier-Lavigne, M., Sotelo, C. and Chédotal, A. (1999). Slit2-Mediated chemorepulsion and collapse of developing forebrain axons. *Neuron* **22**, 463-473.

Nobes, C. D. and Hall, A. (1995). Rho, rac, and cdc42 GTPases regulate the assembly of multimolecular focal complexes associated with actin stress fibers, lamellipodia, and filopodia. *Cell* **81**, 53-62.

Okada, M. and Nakagawa, H. (1989). A protein tyrosine kinase involved in regulation of pp60c-src function. *J. Biol. Chem.* **264**, 20886-20893.

Pelish, H. E., Peterson, J. R., Salvarezza, S. B., Rodriguez-Boulan, E., Chen, J. L., Stamnes, M., Macia, E., Feng, Y., Shair, M. D. and Kirchhausen, T. (2006). Secramine inhibits Cdc42-dependent functions in cells and Cdc42 activation in vitro. *Nat. Chem. Biol.* **2**, 39-46.

Peng, J., Wallar, B. J., Flanders, A., Swiatek, P. J. and Alberts, A. S. (2003). Disruption of the Diaphanous-related formin Drf1 gene encoding mDia1 reveals a role for Drf3 as an effector for Cdc42. *Curr. Biol.* **13**, 534-545.

Pertz, O. C., Wang, Y., Yang, F., Wang, W., Gay, L. J., Gristenko, M. A., Clauss, T. R., Anderson, D. J., Liu, T., Auberry, K. J. et al. (2008). Spatial mapping of the neurite and soma proteomes reveals a functional Cdc42/Rac regulatory network. *Proc. Natl. Acad. Sci. USA* **105**, 1931-1936.

Ren, X. D., Kiosses, W. B., Sieg, D. J., Otey, C. A., Schlaepfer, D. D. and Schwartz, M. A. (2000). Focal adhesion kinase suppresses Rho activity to promote focal adhesion turnover. *J. Cell Sci.* **113**, 3673-3678.

Ren, X. R., Ming, G. L., Xie, Y., Hong, Y., Sun, D. M., Zhao, Z. Q., Feng, Z., Wang, Q., Shim, S., Chen, Z. F. et al. (2004). Focal adhesion kinase in netrin-1 signaling. *Nat. Neurosci.* **7**, 1204-1212.

Rohatgi, R., Ho, H. Y. and M. W. Kirschner (2000). Mechanism of N-WASP activation by CDC42 and phosphatidylinositol 4, 5-bisphosphate. *J. Cell Biol.* **150**, 1299-1310.

Rico, B., Beggs, H. E., Schahin-Reed, D., Kimes, N., Schmidt, A. and Reichardt, L. F. (2004). Control of axonal branching and synapse formation by focal adhesion kinase. *Nat. Neurosci.* **7**, 1059-1069.

Robles, E. and Gomez, T. M. (2006). Focal adhesion kinase signaling at sites of integrin-mediated adhesion controls axon pathfinding. *Nat Neurosci.* **9**, 1274-1283.

Robles, E., Woo, S. and Gomez, T. M. (2005). Src-dependent tyrosine phosphorylation at the tips of growth cone filopodia promotes extension. *J. Neurosci.* **25**, 7669-7681.

Schaller, M. D., Borgman, C. A. and Parsons, J. T. (1993). Autonomous expression of a noncatalytic domain of the focal adhesion-associated protein tyrosine kinase pp125FAK. *Mol. Cell. Biol.* **13**, 785-791.

Schaller, M. D., Hildebrand, J. D., Shannon, J. D., Fox, J. W., Vines, R. R. and Parsons, J. T. (1994). Autophosphorylation of the focal adhesion kinase, pp125FAK, directs SH2-dependent binding of pp60src. *Mol. Cell. Biol.* **14**, 1680-1688.

Shekarabi, M., Moore, S. W., Tritsch, N. X., Morris, S. J., Bouchard, J. F. and Kennedy, T. E. (2005). Deleted in colorectal cancer binding netrin-1 mediates cell substrate adhesion and recruits Cdc42, Rac1, Pak1, and N-WASP into an intracellular signaling complex that promotes growth cone expansion. *J. Neurosci.* **25**, 3132-3141.

Slack-Davis, J. K., Martin, K. H., Tilghman, R. W., Iwanicki, M., Ung, E. J., Autry, C., Luzzio, M. J., Cooper, B., Kath, J. C., Roberts, W. G. et al. (2007). Cellular characterization of a novel focal adhesion kinase inhibitor. *J. Biol. Chem.* **282**, 14845-14852.

Sokac, A. M., Co, C., Taunton, J. and Bement, W. (2003). Cdc42-dependent actin polymerization during compensatory endocytosis in Xenopus eggs. *Nat. Cell Biol.* **5**, 727-732.

Stein, E. and Tessier-Lavigne, M. (2001). Hierarchical organization of guidance receptors: silencing of netrin attraction by slit through a Robo/DCC receptor complex. *Science* **291**, 1928-1938.

Thomas, S. M. and Brugge, J. S. (1997). Cellular functions regulated by Src family kinases. *Annu. Rev. Cell Dev. Biol.* **13**, 513-609.

Torres, E. and Rosen, M. K. (2003). Contingent phosphorylation/dephosphorylation provides a mechanism of molecular memory in WASP. *Mol. Cell* **11**, 1215-1227.

Västrik, I., Eickholt, B. J., Walsh, F. S., Ridley, A. and Doherty, P. (1999). Sema3A-induced growth-cone collapse is mediated by Rac1 amino acids 17-32. *Curr. Biol.* **9**, 991-998.

Ward, M. E., Wu, J. Y. and Rao, Y. (2004). Visualization of spatially and temporally regulated N-WASP activity during cytoskeletal reorganization in living cells. *Proc. Natl. Acad. Sci. USA* **101**, 970-974.

Welch, M. D. (1999). The world according to Arp: regulation of actin nucleation by the Arp2/3 complex. *Trends Cell Biol.* **9**, 423-427.

Weston, C. A., Anova, L., Rialas, C., Prives, J. M. and Weeks, B. S. (2000). Laminin-1 activates Cdc42 in the mechanism of laminin-1-mediated neurite outgrowth. *Exp. Cell Res.* **260**, 374-378.

Wong, K., Ren, X. R., Huang, Y. Z., Xie, Y., Liu, G., Saito, H., Tang, H., Wen, L., Brady-Kalnay, S. M., Mei, L. et al. (2001). Signal transduction in neuronal migration: roles of GTPase activating proteins and the small GTPase Cdc42 in the Slit-Robo pathway. *Cell* **107**, 209-221.

Woo, S., Rowan, D. J. and Gomez, T. M. (2009). Retinotopic mapping requires focal adhesion kinase-mediated regulation of growth cone adhesion. *J. Neurosci.* **29**, 13981-13991.

Yuan, X. B., Jin, M., Xu, X., Song, Y. Q., Wu, C. P., Poo, M. M. and Duan, S. (2003). Signalling and crosstalk of Rho GTPases in mediating axon guidance. *Nat. Cell Biol.* **5**, 38-45.

Zheng, J. Q., Wan, J. J. and Poo, M. M. (1996). Essential role of filopodia in chemotropic turning of nerve growth cone induced by a glutamate gradient. *J. Neurosci.* **16**, 1140-1149.